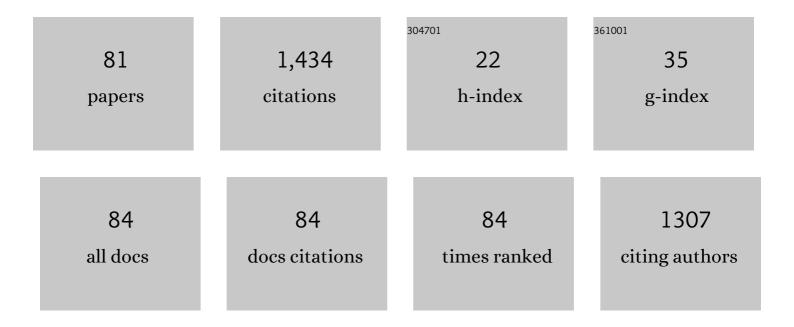
Tae-Hyuk Kwon

List of Publications by Year in descending order

Source: https://exaly.com/author-pdf/3166730/publications.pdf Version: 2024-02-01



TAE-HVILK KWON

#	Article	IF	CITATIONS
1	Review on geotechnical engineering properties of sands treated by microbially induced calcium carbonate precipitation (MICP) and biopolymers. Construction and Building Materials, 2020, 246, 118415.	7.2	155
2	Gas hydrate dissociation in sediments: Pressureâ€ŧemperature evolution. Geochemistry, Geophysics, Geosystems, 2008, 9, .	2.5	100
3	Improvement of Surface Erosion Resistance of Sand by Microbial Biopolymer Formation. Journal of Geotechnical and Geoenvironmental Engineering - ASCE, 2018, 144, .	3.0	65
4	Geotechnical properties of deep oceanic sediments recovered from the hydrate occurrence regions in the Ulleung Basin, East Sea, offshore Korea. Marine and Petroleum Geology, 2011, 28, 1870-1883.	3.3	61
5	Observations of poreâ€scale growth patterns of carbon dioxide hydrate using <scp>X</scp> â€ray computed microtomography. Geochemistry, Geophysics, Geosystems, 2015, 16, 912-924.	2.5	55
6	Effect of Electric Field on Gas Hydrate Nucleation Kinetics: Evidence for the Enhanced Kinetics of Hydrate Nucleation by Negatively Charged Clay Surfaces. Environmental Science & Technology, 2018, 52, 3267-3274.	10.0	48
7	Surface-erosion behaviour of biopolymer-treated soils assessed by EFA. Geotechnique Letters, 2020, 10, 106-112.	1.2	45
8	Depressurizationâ€Induced Fines Migration in Sediments Containing Methane Hydrate: Xâ€Ray Computed Tomography Imaging Experiments. Journal of Geophysical Research: Solid Earth, 2018, 123, 2539-2558.	3.4	42
9	Observation of the Degradation Characteristics and Scale of Unevenness on Three-dimensional Artificial Rock Joint Surfaces Subjected to Shear. Rock Mechanics and Rock Engineering, 2016, 49, 3-17.	5.4	38
10	Effect of Pore Size Distribution on Dissociation Temperature Depression and Phase Boundary Shift of Gas Hydrate in Various Fine-Grained Sediments. Energy & Fuels, 2018, 32, 5321-5330.	5.1	38
11	Destabilization of Marine Gas Hydrate-Bearing Sediments Induced by a Hot Wellbore: A Numerical Approach. Energy & Fuels, 2010, 24, 5493-5507.	5.1	33
12	Effect of slit-type barrier on characteristics of water-dominant debris flows: small-scale physical modeling. Landslides, 2018, 15, 111-122.	5.4	31
13	Microbial community analyses of produced waters from highâ€ŧemperature oil reservoirs reveal unexpected similarity between geographically distant oil reservoirs. Microbial Biotechnology, 2018, 11, 788-796.	4.2	31
14	Modification of Interfacial Tension and Wettability in Oil–Brine–Quartz System by in Situ Bacterial Biosurfactant Production at Reservoir Conditions: Implications for Microbial Enhanced Oil Recovery. Energy & Fuels, 2019, 33, 4909-4920.	5.1	30
15	Shear behavior of rectangular-shaped asperities in rock joints. KSCE Journal of Civil Engineering, 2010, 14, 323-332.	1.9	29
16	Thermal Dissociation Behavior and Dissociation Enthalpies of Methane–Carbon Dioxide Mixed Hydrates. Journal of Physical Chemistry B, 2011, 115, 8169-8175.	2.6	29
17	Geomechanical and Thermal Responses of Hydrate-Bearing Sediments Subjected to Thermal Stimulation: Physical Modeling Using a Geotechnical Centrifuge. Energy & Fuels, 2013, 27, 4507-4522.	5.1	29
18	Submarine Slope Failure Primed and Triggered by Bottom Water Warming in Oceanic Hydrate-Bearing Deposits. Energies, 2012, 5, 2849-2873.	3.1	28

ΤΑΕ-ΗΥUK KWON

#	Article	IF	CITATIONS
19	Fines migration and pore clogging induced by single- and two-phase fluid flows in porous media: From the perspectives of particle detachment and particle-level forces. Geomechanics for Energy and the Environment, 2020, 23, 100131.	2.5	28
20	High-frequency seismic response during permeability reduction due to biopolymer clogging in unconsolidated porous media. Geophysics, 2013, 78, EN117-EN127.	2.6	27
21	<i>P</i> and <i>S</i> wave responses of bacterial biopolymer formation in unconsolidated porous media. Journal of Geophysical Research G: Biogeosciences, 2016, 121, 1158-1177.	3.0	26
22	Rheological Properties of Cemented Tailing Backfill and the Construction of a Prediction Model. Materials, 2015, 8, 2076-2092.	2.9	25
23	Assessment of barrier location effect on debris flow based on smoothed particle hydrodynamics (SPH) simulation on 3D terrains. Landslides, 2021, 18, 217-234.	5.4	23
24	Visualization and prediction of supercritical CO2 distribution in sandstones during drainage: An in situ synchrotron X-ray micro-computed tomography study. International Journal of Greenhouse Gas Control, 2017, 66, 230-245.	4.6	21
25	Site characterization and geotechnical aspects on geological storage of CO2 in Korea. Geosciences Journal, 2014, 18, 167-179.	1.2	20
26	Systematic Modeling Approach to Selective Plugging Using <i>In Situ</i> Bacterial Biopolymer Production and Its Potential for Microbial-enhanced Oil Recovery. Geomicrobiology Journal, 2019, 36, 468-481.	2.0	19
27	Dissociation Behavior of CO ₂ Hydrate in Sediments during Isochoric Heating. Environmental Science & Technology, 2008, 42, 8571-8577.	10.0	18
28	Geomechanical, Hydraulic and Thermal Characteristics of Deep Oceanic Sandy Sediments Recovered during the Second Ulleung Basin Gas Hydrate Expedition. Energies, 2016, 9, 775.	3.1	18
29	Long-Term Remote Monitoring of Ground Deformation Using Sentinel-1 Interferometric Synthetic Aperture Radar (InSAR): Applications and Insights into Geotechnical Engineering Practices. Applied Sciences (Switzerland), 2020, 10, 7447.	2.5	18
30	Photoelastic observation of toughness-dominant hydraulic fracture propagation across an orthogonal discontinuity in soft, viscoelastic layered formations. International Journal of Rock Mechanics and Minings Sciences, 2020, 134, 104438.	5.8	17
31	Xâ€Ray Computed Microtomography Imaging of Abiotic Carbonate Precipitation in Porous Media From a Supersaturated Solution: Insights Into Effect of CO ₂ Mineral Trapping on Permeability. Water Resources Research, 2019, 55, 3835-3855.	4.2	16
32	Evolution of Compressional Wave Velocity during CO ₂ Hydrate Formation in Sediments. Energy & Fuels, 2009, 23, 5731-5736.	5.1	15
33	Biosurfactant as an Enhancer of Geologic Carbon Storage: Microbial Modification of Interfacial Tension and Contact Angle in Carbon dioxide/Water/Quartz Systems. Frontiers in Microbiology, 2017, 8, 1285.	3.5	15
34	Auto-detection of acoustic emission signals from cracking of concrete structures using convolutional neural networks: Upscaling from specimen. Expert Systems With Applications, 2021, 186, 115863.	7.6	15
35	Ultrasonic P-Wave Reflection Monitoring of Soil Erosion for Erosion Function Apparatus. Geotechnical Testing Journal, 2016, 39, 301-314.	1.0	15
36	Effect of CO ₂ hydrate formation on seismic wave velocities of fineâ€grained sediments. Geochemistry, Geophysics, Geosystems, 2013, 14, 1787-1799.	2.5	14

ΤΑΕ-ΗΥUK KWON

#	Article	IF	CITATIONS
37	Modeling of Permeability Reduction in Bioclogged Porous Sediments. Journal of Geotechnical and Geoenvironmental Engineering - ASCE, 2018, 144, .	3.0	14
38	Effect of Moisture Content and Particle Size on Extinction Coefficients of Soils Using Terahertz Time-Domain Spectroscopy. IEEE Transactions on Terahertz Science and Technology, 2017, 7, 529-535.	3.1	13
39	Effect of Partial Water Saturation on Attenuation Characteristics of Low Porosity Rocks. Rock Mechanics and Rock Engineering, 2011, 44, 245-251.	5.4	11
40	Effect of Fluid–Rock Interactions on In Situ Bacterial Alteration of Interfacial Properties and Wettability of CO ₂ –Brine–Mineral Systems for Geologic Carbon Storage. Environmental Science & Technology, 2020, 54, 15355-15365.	10.0	11
41	The emerging role of 4D synchrotron X-ray micro-tomography for climate and fossil energy studies: five experiments showing the present capabilities atÂbeamline 8.3.2 at the Advanced Light Source. Journal of Synchrotron Radiation, 2017, 24, 1237-1249.	2.4	10
42	Experimental investigation on the variation of thermal conductivity of soils with effective stress, porosity, and water saturation. Geomechanics and Engineering, 2016, 11, 771-785.	0.9	10
43	Characteristics of steady-state propagation of hydraulic fractures in ductile elastic and two-dimensionally confined plate media. International Journal of Rock Mechanics and Minings Sciences, 2019, 114, 164-174.	5.8	9
44	Smart geophysical characterization of particulate materials in a laboratory. Smart Structures and Systems, 2005, 1, 217-233.	1.9	9
45	Grain-Scale Tensile and Shear Strengths of Glass Beads Cemented by MICP. Journal of Geotechnical and Geoenvironmental Engineering - ASCE, 2022, 148, .	3.0	9
46	Effects of bacterial dextran on soil geophysical properties. Environmental Geotechnics, 2018, 5, 114-122.	2.3	8
47	An Integrated Approach to Real-Time Acoustic Emission Damage Source Localization in Piled Raft Foundations. Applied Sciences (Switzerland), 2020, 10, 8727.	2.5	7
48	Preliminary report of a catastrophic landslide that occurred in Gokseong County, South Jeolla Province, South Korea, on August 7, 2020. Landslides, 2021, 18, 1465-1469.	5.4	7
49	Measuring elastic modulus of bacterial biofilms in a liquid phase using atomic force microscopy. Geomechanics and Engineering, 2017, 12, 863-870.	0.9	7
50	Study on Viscous Fluid Flow in Disordered-Deformable Porous Media Using Hydro-mechanically Coupled Pore-Network Modeling. Transport in Porous Media, 2020, 133, 207-227.	2.6	6
51	Use of a Pre-Drilled Hole for Implementing Thermal Needle Probe Method for Soils and Rocks. Energies, 2016, 9, 846.	3.1	5
52	Sensitivity analysis of influencing parameters on slit-type barrier performance against debris flow using 3D-based numerical approach. International Journal of Sediment Research, 2021, 36, 50-62.	3.5	5
53	A Newly Developed State-of-the-Art Full-Scale Excavation Testing Apparatus for Tunnel Boring Machine (TBM). KSCE Journal of Civil Engineering, 2021, 25, 4856-4867.	1.9	5
54	In situ viscoelastic properties of insoluble and porous polysaccharide biopolymer dextran produced by Leuconostoc mesenteroides using particle-tracking microrheology. Geomechanics and Engineering, 2017, 12, 849-862.	0.9	5

ΤΑΕ-ΗΥϤΚ Κ₩ΟΝ

#	Article	IF	CITATIONS
55	Microbiology and Microbial Products for Enhanced Oil Recovery. , 2020, , 27-65.		4
56	Entrapment of clay particles enhances durability of bacterial biofilm-associated bioclogging in sand. Acta Geotechnica, 2022, 17, 119-129.	5.7	4
57	Relaxation behavior in low-frequency complex conductivity of sands caused by bacterial growth and biofilm formation by <i>Shewanella oneidensis</i> under a high-salinity condition. Geophysics, 2021, 86, B389-B400.	2.6	4
58	Effect of Soft Viscoelastic Biopolymer on the Undrained Shear Behavior of Loose Sands. Journal of Geotechnical and Geoenvironmental Engineering - ASCE, 2021, 147, .	3.0	4
59	An experimental procedure for evaluating the consolidation state of marine clay deposits using shear wave velocity. Smart Structures and Systems, 2011, 7, 289-302.	1.9	4
60	Seismic monitoring of permeability reduction due to biopolymer formation in unconsolidated materials. , 2011, , .		3
61	Study of Korea Early Warning System for Slope Failure. Korean Society of Hazard Mitigation, 2019, 19, 73-81.	0.2	2
62	Monitoring of Low-Frequency Seismic Responses during Microbial Biofilm and EPS Formations in Unconsolidated Sediments. Environmental Geotechnics, 0, , 1-10.	2.3	2
63	Preliminary Study of Geophysical Monitoring of Bioclogging Caused by Bacterial Biopolymer Accumulation in Sands. , 2014, , .		1
64	Diffusive and Convective Transport of Disposed CO ₂ in Porous Media: A Numerical Approach. , 2014, , .		1
65	Analysis of laboratory data on ultrasonic monitoring of permeability reduction due to biopolymer formation in unconsolidated granular media. Geophysical Prospecting, 2016, 64, 445-455.	1.9	1
66	Hydromechanical responses of coal powders by CO2 adsorption. Environmental Geotechnics, 2017, 4, 94-102.	2.3	1
67	Video data of hydraulic fracture propagation in two-dimensionally confined gelatin plates. Data in Brief, 2019, 25, 104096.	1.0	1
68	Theory and Experiments. , 2020, , 67-108.		1
69	A small pore size effect on dissociation behavior of gas hydrates in fine-grained sediments. , 2016, , 459-462.		1
70	A Case Study on the Closed-Type Barrier Effect on Debris Flows at Mt. Woomyeon, Korea in 2011 via a Numerical Approach. Energies, 2021, 14, 7890.	3.1	1
71	Effect of Salt Water on the Process of Microbially Induced Carbonate Precipitation. , 2022, , .		1
72	Characterization of soil properties using elastic and electromagnetic waves. , 2003, 5057, 440.		0

72 Characterization of soil properties using elastic and electromagnetic waves. , 2003, 5057, 440.

ΤΑΕ-ΗΥϤΚ Κ₩ΟΝ

#	Article	IF	CITATIONS
73	Roles of spacing and angle of slit-type barriers on velocity reduction of debris flows. Japanese Geotechnical Society Special Publication, 2016, 2, 963-966.	0.2	0
74	Preliminary study on P-wave monitoring of soil erosion in SRICOS-EFA method. Japanese Geotechnical Society Special Publication, 2016, 2, 1757-1760.	0.2	0
75	The Production-Induced Geomechanical Property Changes during Gas Production from Gas Hydrate Deposits. , 2019, , .		0
76	Impact of Interbedded Structure of Sand and Clay Layers on Geomechanical Responses of Hydrate-Bearing Sediments During Depressurization. , 2019, , .		0
77	Modeling and Simulation. , 2020, , 109-168.		0
78	MONITORING OF CO2 HYDRATE FORMATION IN SEDIMENTS USING COMPRESSIONAL WAVE VELOCITY. , 2008, , .		0
79	Interactions between hydraulic fracture and interfaces in layered formations. , 2016, , 217-221.		0
80	Numerical Computation of Hydraulic Conductivity of Sand Using X-ray Microtomography Imaging of a Pore Structure. Korean Society of Hazard Mitigation, 2019, 19, 187-192.	0.2	0
81	Fluid-driven mechanical responses of deformable porous media during two-phase flows: Hele-Shaw experiments and hydro-mechanically coupled pore network modeling. E3S Web of Conferences, 2020, 205, 08009.	0.5	0